EUROPEAN ORGANIZATION FOR NUCLEAR RESEARCH

Proposal to the ISOLDE and Neutron Time-of-Flight Committee

Laser assisted studies of β-delayed fission in ^{178,176}Au and of the structure of ^{175}Au

May 13, 2020

B. Andel[1,2], A. N. Andreyev[3], S. Antalic[2], A. E. Barzakh[4], T. Berry[5], M. J. G. Borge[6], J. A. Briz[6], A. Broniš[2], T. E. Cocolios[1], K. Chrysalidis[7], J. G. Cubiss[3], H. De Witte[1], K. Dockx[1], D. V. Fedorov[4], V. N. Fedosseev[7], L. M. Fraile[8], H. O. U. Fynbo[9], P. T. Greenlees[10], L. J. Harkness-Brennan[11], R. Heinke[1], J. Johnson[1], D. T. Joss[11], D. S. Judson[11], J. Konki[10], J. Kurcewicz[7], I. Lazarus[12], R. Lică[13], M. Madurga[7], N. Marginean[13], B. A. Marsh[7], C. Mihai[13], P. L. Molkanov[4], P. Mosat[2], E. Nacher[14], A. Negret[13], K. Nishio[15], R. D. Page[11], S. Pascu[13], A. Perea[6], V. Pucknell[12], P. Rahkila[10], E. Rapisarda[7], M. D. Seliverstov[4], A. Sott[3], C. Sotty[13], P. Spagnoletti[16], M. Stryjczyk[1], O. Tengblad[6], I. Tsekhanovich[17], P. Van Duppen[1], V. Vedia[8], R. Wadsworth[3], N. Warr[18], and S. G. Wilkins[7]

[1] *KU Leuven, Instituut voor Kern- en Stralingsfysica, 3001 Leuven, Belgium*
[2] *Department of Nuclear Physics and Biophysics, Comenius University in Bratislava, 84248 Bratislava, Slovakia*
[3] *Department of Physics, University of York, Heslington, York, YO10 5DD, United Kingdom*
[4] *Petersburg Nuclear Physics Institute, NRC Kurchatov Institute, 188300 Gatchina, Russia*
[5] *Department of Physics, University of Surrey, Guildford GU2 7XH, United Kingdom*
[6] *Instituto de Estructura de la Materia, CSIC, Serrano 113 bis, E-28006 Madrid, Spain*
[7] *CERN, CH-1211 Geneve 23, Switzerland*
[8] *Grupo de Física Nuclear, Universidad Complutense de Madrid, 28040, Madrid, Spain*
[9] *Department of Physics and Astronomy, Aarhus University, DK-8000 Aarhus C, Denmark*
[10] *University of Jyväskylä, Department of Physics, P.O. Box 35, FI-40014, Jyväskylä, Finland*
[11] *Department of Physics, Oliver Lodge Laboratory, University of Liverpool, Liverpool L69 7ZE, United Kingdom*
[12] *STFC Daresbury, Daresbury, Warrington WA4 4AD, United Kingdom*
[13] *"Horia Hulubei" National Institute for R & D in Physics and Nuclear Engineering, RO-077125 Bucharest, Romania*
[14] *Instituto de Física Corpuscular, CSIC - Universidad de Valencia, E-46980, Valencia, Spain*
[15] *Advanced Science Research Center, JAEA, Tokai, Ibaraki 319-1195, Japan*
[16] *Simon Fraser University, Burnaby, Canada*
[17] *CENBG, Bordeaux, France*
[18] *Institut für Kernphysik, Universität zu Köln, 50937 Köln, Germany*

Spokespersons: B. Andel [boris.andel@kuleuven.be]
A. N. Andreyev [andrei.andreyev@york.ac.uk]
A. E. Barzakh [barzakh@mail.ru]
J. G. Cubiss [james.cubiss@york.ac.uk]
P. Van Duppen [piet.vanduppen@kuleuven.be]
Contact person: R. Lică [razvan.lica@cern.ch]

Abstract: The gold isotopes (Au, $Z = 79$) are especially well suited for the study of β-delayed fission (βDF) and shape coexistence in exotic nuclei. The proposed measurements aim at the identification of βDF in ^{178,176}Au, employing RILIS-ionized isomerically separated beams of their high- and low-spin states, thus allowing studies of scarcely-known spin-dependence of fission properties. The measurement of fission fragment energies of ^{178}Pt (β-decay daughter of ^{178}Au) will allow the predicted island of fragment mass asymmetry below $Z = 82$ to be probed. The proposed investigation of the hyperfine structure (hfs) and isotope shift of ^{175}Au ground state (gs) will provide the first information on its mean-square charge radius and g-factor, which will allow us to determine its configuration. The character of this state is of high interest, since according to the spherical shell model, a $\pi 2d_{3/2}$ configuration is expected, while the trend in g-factors of ^{177,179}Au^{gs} and unhindered α decay of ^{179}Tl^{gs} $\rightarrow$ ^{175}Au^{gs} suggest a nearly pure intruder $\pi 3s_{1/2}$ state. The latter configuration in ^{175}Au^{gs} would indicate a rearranging of spherical shell model states in the lightest gold isotopes.

Requested shifts: 14 shifts with UC_x target (in a single run)

1 β-delayed fission of ^{178}Au^{gs,is} and ^{176}Au^{gs,is}

1.1 Motivation and goals

Beta-delayed fission (βDF) provides wealth of information on low-energy fission of exotic isotopes [1] and has an important impact on the production of elements in nucleosynthesis [2, 3]. Both the βDF probability ($P_{\beta DF}$) and the fission fragment mass distributions (FFMDs) play an important role in the final abundancies of isotopes via fission recycling in the r-process [4]. However, neutron-rich nuclei crucial for r-process are currently inaccessible for experimental studies. Therefore, to guide and validate theoretical fission developments in these unknown regions, βDF can be studied in more accessible, neutron-deficient regions of the nuclear chart. Nonetheless, the experimental information, which could help to benchmark models, remains scarce. For example, the specific $P_{\beta DF}$ value was determined only for 17 cases [5, 6] and FFMDs were reported for 12 nuclei [7, 8] so far.

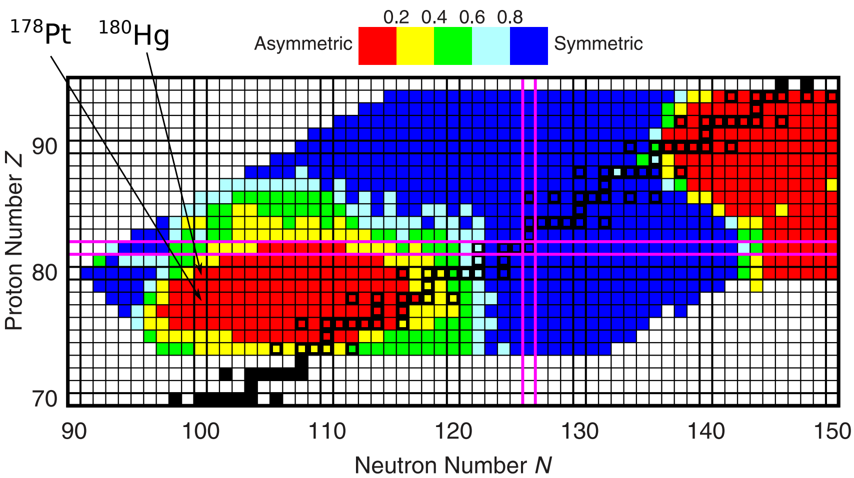

Figure 1: The predictions of asymmetric and symmetric low-energy fission for nuclei with Z = 70–95, taken from [12]. The two regions of asymmetric fission are shown in red: the classical asymmetric fission in heavy actinides is in the top-right corner, the newly-established region below Z = 82 is in the bottom-left with an area of symmetric fission in between (blue). The asymmetrically fissioning ^{180}Hg is situated at the predicted border of the new region of asymmetry, while ^{178}Pt is located farther inside the region (both isotopes are marked by arrows).

In the neutron-deficient lead region, βDF measurements performed by our collaboration at ISOLDE established a new region of asymmetric fission through the surprising discovery of asymmetric mass split of ^{180,178}Hg, β-decay daughters of ^{180,178}Tl [9, 10, 11]. This discovery generated a high interest from the theory side [7]. Figure. 1 shows global FFMD calculations from Ref. [12], which predicted the existence of a broad, new region of asymmetric fission below $Z = 82$.

Experimentally, the extent of this island of asymmetry below ^{180,178}Hg ($Z = 80$) remains unknown. Information is only available for fission at higher excitation energies ($E^* = 40$–60 MeV) from complete-fusion reaction experiments, where competition of symmetric and asymmetric fission was observed for the compound nuclei ^{179}Au [13] and ^{178}Pt [14]. A predominant asymmetric component in FFMD of ^{178}Pt, which still survives at high E^* values [14], suggests that low-energy fission such as βDF (with $E^* \lesssim 10$ MeV) can be expected to be fully asymmetric.

The proposed βDF studies of ^{178}Au will provide the low-energy fission data for ^{178}Pt (β-decay daughter of ^{178}Au), which will probe deeper into the predicted island of asymmetric fission. We will identify and study βDF separately for the ground (gs) and isomeric (is) state in ^{178}Au and in ^{176}Au by employing isomerically separated beams supplied by RILIS at ISOLDE. Our recent experiment demonstrated that the ground and isomeric states in ^{178,176}Au are well separeted in hyperfine spectrum (hfs) [15, 16] and their selective ionization can be achieved even in broadband mode of RILIS (example of hfs for ^{178}Au is shown in Fig. 2). Thus, there will be no loss in production yields, typical for the use of higher-resolution narrowband mode. Spins $I(^{178}\mathrm{Au}^{\mathrm{gs}}) = (2, 3)$, $I(^{178}\mathrm{Au}^{\mathrm{is}}) = (7, 8)$ and β-decay branching ratios for $^{178}\mathrm{Au}^{\mathrm{gs,is}}$, $^{176}\mathrm{Au}^{\mathrm{gs,is}}$ were also deduced [15, 16].

To estimate the expected fission rate, we used the systematics of known $P_{\beta\mathrm{DF}}$ values as a function of the difference $Q_\beta - B_f$ (Fig. 3), where Q_β is the Q value of the β decay of the mother and B_f is the fission barrier height of the daughter nucleus. Two widely used aprroaches for B_f calculations, the Thomas-Fermi model (TF) [18] and Finite-Range Liquid-Drop Model (FRLDM) [19], were employed and systematics based on them show an exponential dependence. However, estimates based on the two systematics lead to almost 3 orders-of-magnitude difference in expected fission fragment (FF) yields for $^{178}\mathrm{Au}^{\mathrm{gs,is}}$ (Table 1). The proposed βDF measurement will therefore provide unique opportunity to resolve validity of these vastly different predictions and the measurements of $P_{\beta\mathrm{DF}}$ alone will allow us to estimate the fission barrier of ^{176,178}Pt, as demonstrated in [17] and references therein.

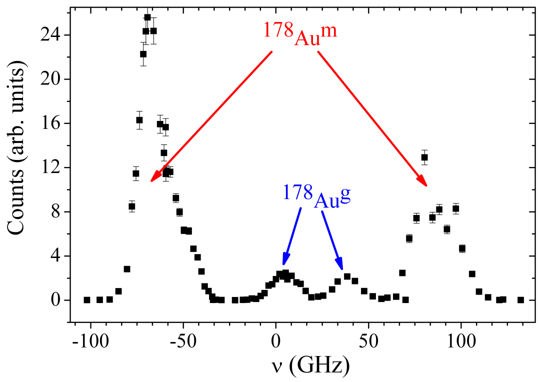

Figure 2: Example of hfs for ^{178}Au measured in broadband mode. Components belonging to ground ($^{178}\mathrm{Au}^{\mathrm{g}}$) and isomeric state ($^{178}\mathrm{Au}^{\mathrm{m}}$) are well separated. Similar well separated pattern was measured also for $^{176}\mathrm{Au}^{\mathrm{gs,is}}$.

If the FF yields for βDF of $^{178}\mathrm{Au}^{\mathrm{gs,is}}$ lie between TF and FRLDM estimates, we will collect $\gtrsim$ 100 FFs for each of the states, which should be sufficient to deduce whether the FFMD is symmetric or asymmetric. This is based on the fact that the inverse ratio

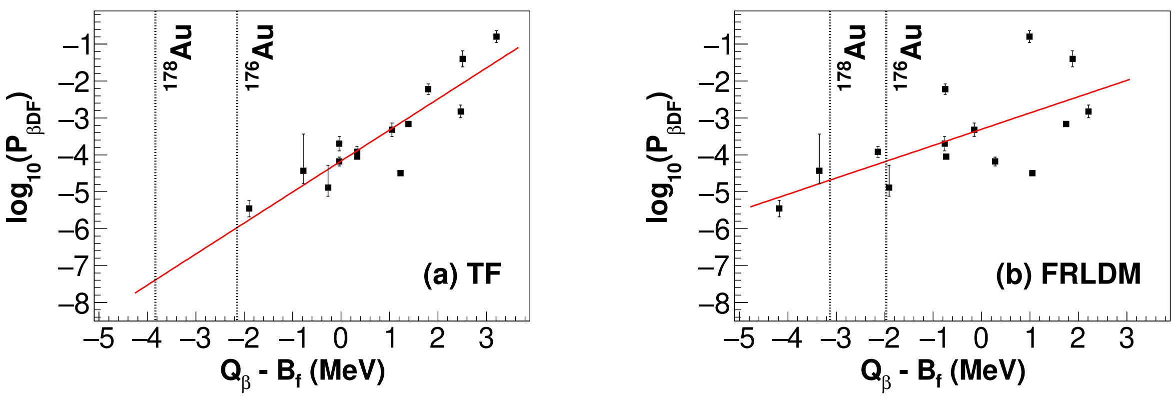

Figure 3: Systematics of $P_{\beta\mathrm{DF}}$ values as a function of $Q_\beta - B_f$, where the B_f values are taken from TF model [18] (a) and FRLDM [19] (b). Q_β values are taken from [20]. Solid red lines show fits to the data with equal weights to all points, dashed vertical lines show $Q_\beta - B_f$ values for ^{178}Au and ^{176}Au. The systematics only include $P_{\beta\mathrm{DF}}$ values for cases considered as reliable in [1, 5] and newer values from [6].

	ions/s	FF/day	
		TF	FRLDM
^{178}Au^{gs}	2.4×10^3	3	1.4×10^3
^{178}Au^{is}	2.0×10^4	23	1.2×10^4
^{176}Au^{gs}	10	0.2	10
^{176}Au^{is}	20	0.5	31

Table 1: Expected implantation rate of isomerically separated ions (using broadband mode of RILIS) at the experimental setup based on our previous measurements, and estimated numbers of FFs detected at IDS per day for βDF of ^{178}Au^{gs,is} and ^{176}Au^{gs,is} based on $P_{\beta DF}$ systematics (Fig. 3).

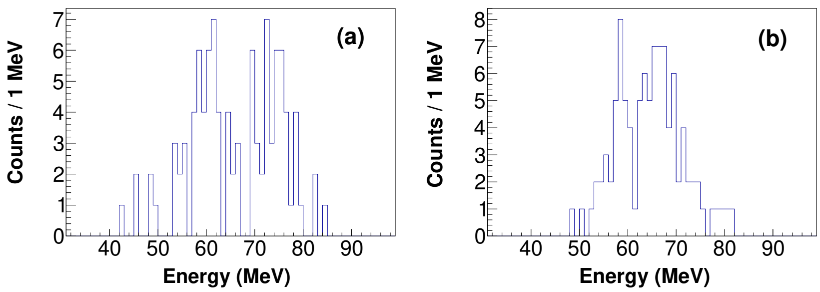

Figure 4: Distribution of 100 randomly selected FF energies from (a) data for ^{180}Tl βDF [10] and (b) Gaussian distribution to simulate symmetric fission.

of FF energies is proportional to ratio of their masses. To illustrate this, Fig. 4(a) shows an example of energy distribution for 100 randomly selected FF events from ^{180}Tl βDF data [10] (asymmetric fission) and Fig. 4(b) shows 100 randomly selected events from single Gaussian distribution with FWHM = 15 MeV (to simulate symmetric fission). The FWHM of peaks for full statistics of ^{180}Tl βDF was $\approx$ 11.5 MeV [10].
By measuring βDF for isomerically separated ^{178}Au^{gs} and ^{178}Au^{is}, we aim to also study the poorly known spin-dependence of fission, both by determination of $P_{\beta DF}$ values and by characterizing the FFMD in each case. Recently, we performed similar βDF investigation with the use of isomerically separated beams of ^{188}Bi^{gs,is} [8].
Additionally, we will attempt to identify βDF also for ^{176}Au^{gs,is}, again employing isomerically separated beams, and to determine respective $P_{\beta DF}$ values. For these states, FF yield estimates based on the two models differ by almost 2 orders of magnitude (Table 1), therefore even with low statistics it would still be possible to test the models.

1.2 Beam request

Considering the estimated yields (Table 1), we request 5 shifts for βDF measurement of ^{178}Au^{gs}, 2 shifts for βDF study of ^{178}Au^{is} and 3 shifts for identification of βDF in ^{176}Au^{gs,is}. We will determine $P_{\beta DF}$ values for investigated states and measure FF energies from which we can deduce if FFMD of ^{178}Pt is symmetric or asymmetric, provided sufficient statistics are collected. The detection setup is described in Sec. 3.

2 Laser spectroscopy of ^{175}Au

2.1 Motivation and goals

Previously, our collaboration performed a successful IS534 campaign of isotope shift (IS) and hfs measurements of neutron-deficient isotopes $^{176-183}$Au, using the in-source laser

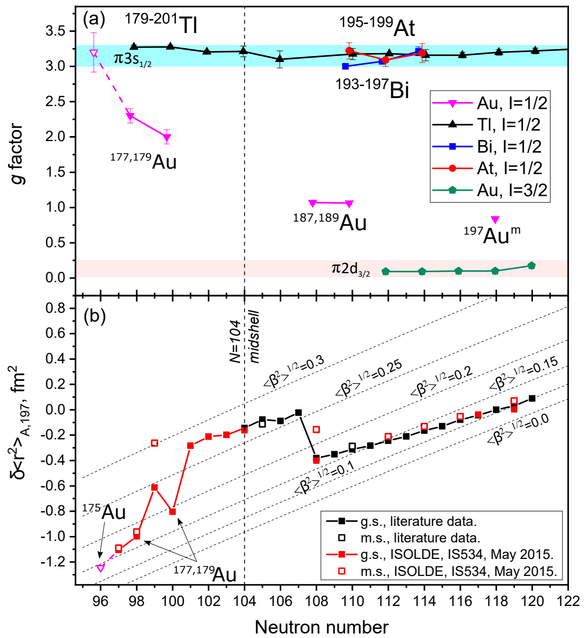

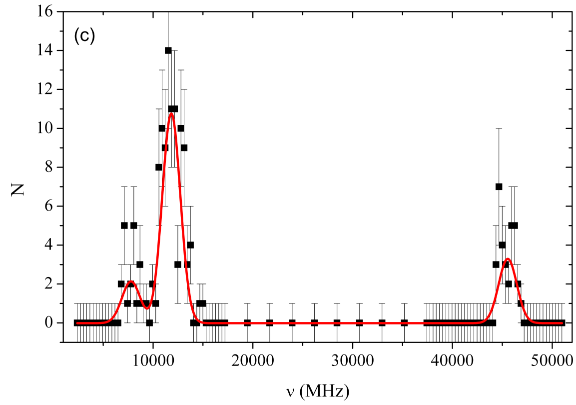

Figure 5: (a) Nuclear g-factors, for $I = 1/2$ ground and isomeric states of isotopes surrounding the $Z = 82$ shell closure, along with the $I = 1/2$ (pink, downwards triangles) and $I = 3/2$ (green diamonds) states in gold isotopes. The blue and pink shaded regions represent the approximate g-factor values for near-pure $\pi 3s_{1/2}$ and $\pi 2d_{3/2}$ states, respectively. Values for g(^{177,179}Au^{gs}) are from our recent work [22] and a hollow triangle shows expected value (with 9% uncertainty) for pure $\pi 3s_{1/2}$ configuration of ^{175}Au^{gs}. (b) Changes in mean-square charge radii of gold isotopes, as a function of neutron number, taken from [27]. (c) An arbitrary subset of the experimental hfs for ^{177}Au^{gs} [22] with reduced statistics, similar to those expected from the measurement of ^{175}Au^{gs}. The data are fitted with Voigt profiles (red line).

spectroscopy technique [21]. Some of the results were presented in recent publications [22, 23, 24]. The aim of this part of the experiment will be to measure the IS and hfs of ^{175}Au^{gs} (and thus, the g-factor) in order to probe the purity of its configuration.

According to the spherical shell model, odd-A gold isotopes are expected to have $I^\pi = 3/2^+$ ground states as the 79$^{\text{th}}$ proton should occupy the $\pi 2d_{3/2}$ orbital. This was confirmed in ^{191,193,195,197}Au^{gs}, which have nearly spherical shapes and pure $\pi 2d_{3/2}$ configurations as shown in Fig. 5(a) (see [22] and references therein). However, the ground states of ^{187,189}Au were found to have $I^\pi = 1/2^+$ with mixed $\pi 3s_{1/2}/\pi 2d_{3/2}$ configurations, as evidenced by their g-factors which lie between the values for pure $\pi 3s_{1/2}$ and $\pi 2d_{3/2}$ single-particle states, see Fig. 5(a).

In our IS534 studies of ^{177,179}Au^{gs} ($N = 98$, 100) we determined I(^{177,179}Au^{gs}) $= 1/2$ for the first time. Furthermore, we found that like ^{187,189}Au, g($1/2^+$,^{177,179}Au^{gs}) indicate a similar, mixed $\pi 3s_{1/2}/\pi 2d_{3/2}$ nature, with a trend towards a purer $\pi 3s_{1/2}$ configuration with decreasing neutron number [22]. The mixed ^{177}Au ground state is also evidenced by the hindered nature of the ^{181}Tl($I^\pi = 1/2^+$, $\pi 3s_{1/2}$) $\rightarrow$^{177}Au^{gs}($I^\pi = 1/2^+$, $\pi 3s_{1/2}/\pi 2d_{3/2}$) α decay [22].

Compared to ^{181}Tl decay, the unhindered ^{179}Tl($I^\pi = 1/2^+$, $\pi 3s_{1/2}$) $\rightarrow$^{175}Au^{gs} α decay suggests a pure $\pi 3s_{1/2}$ ground state configuration in ^{175}Au [25]. This assignment cannot be explained by spherical shell model considerations alone, or by the Nilsson model where a $1/2^+$[411] ($3/2^+$[402]) ground state with a dominant $d_{3/2}$ component, at small oblate (prolate) deformation would be expected. Thus, a pure $\pi 3s_{1/2}$ ground-state configuration in ^{175}Au would indicate a rearranging of spherical shell model states in the lightest gold isotopes, far from stability. The expected g-factor for such a pure $\pi 3s_{1/2}$ configuration in ^{175}Au^{gs} is shown by the hollow, pink triangle in Fig. 5(a). To further describe the structure of ^{175}Au^{gs} we need also information about the deformation of this nucleus, which was not measured until now and will be provided by an IS measurement, as was done for heavier gold isotopes [Fig. 5(b)]. Therefore, it is of great importance to perform hfs and IS measurements on ^{175}Au^{gs} in order to deduce its g-factor and charge radius.

2.2 Beam request

We will use the same three-step RILIS ionization process employed in our previous studies [22]. Based on an extrapolation of the production yields observed in $^{176-178}$Au and the half-life of ^{175}Au^{gs} ($T_{1/2}$ = 207(7) ms [25]), we estimate an implantation rate of $\approx$ 0.3 ions/s, which is higher than the lowest rate that we have successfully investigated previously ($\approx$ 0.1 ions/s for ^{177}Hg [26]). Thus, a single hfs scan containing 100 points with a maximum of 15 counts in the peak would require an $\approx$ 4-hour period, with 4 shifts needed to complete 3 full scans. This also includes preliminary RILIS scans in broadband mode in order to locate the hfs of ^{175}Au (1 shift) and then the setup and optimization of RILIS in narrowband mode (1 shift), and reference scans of ^{177,197}Au to optimize and verify the data taking system. The detection setup is described in Sec. 3.
In order to test the feasibility of analyzing the expected data, we downscaled the statistics of two of our ^{177}Au^{gs} hfs scans from [22] to approximately 15 counts in the peak and fitted them independently. An example of one of the fits is shown in Fig. 5(c). Based on this procedure we estimate that our result for g-factor of ^{175}Au^{gs} will have an uncertainty of $\approx$ 9%, as shown in Fig. 5(a), which is sufficient for determination of its configuration.

3 Detection setup

Both the βDF and hfs measurements will be performed at the IDS setup, for which the standard configuration consists of a tape station and 4 HPGe clover detectors. An annular silicon detector will be installed in front of the implantation tape for measurement of α particles and FFs with a geometric efficiency of $\approx$ 20% in a configuration reminiscent of the previous work with the Windmill setup [10]. A plastic scintillator detector will be placed behind the tape to register β particles. The chamber will be surrounded by fast-timing $LaBr_3$ detectors to measure lifetimes of levels populated in β decays ^{178}Au $\rightarrow$ ^{178}Pt as a by-product during the βDF run (no extra beam time required). Most importantly, a lifetime measurement of the 0_2^+ state in ^{178}Pt would allow direct information on the mixing of the two coexisting structures - 0_1^+ and 0_2^+ states to be accessed.
Additionally, an α-decay setup as designed for IS637 will be installed at LA1 and in the case of high fission yields ($\gtrsim$ 100 FFs per shift) it will be used for FFMD measurements in the βDF part of this proposal. The setup contains a movable ladder with 10 thin (20 μg/cm^2) carbon foils, which are transparent for α particles and FFs, and two silicon detectors surrounding the foil at implantation position (the detector closer to beamline is annular). The combined geometric efficiency of the two detectors is $\approx$55%. The configuration enables detection of FF coincidences, which is necessary for a full FFMD

determination as performed in earlier Windmill experiments (see for example Ref. [10]).

Summary of requested shifts: 10 shifts for ^{178,176}Au βDF studies and 4 shifts for ^{175}Au laser spectroscopy with RILIS. In total, 14 shifts employing UC_x target.

References

[1] A. N. Andreyev *et al.*, Rev. Mod. Phys. **85**, 1541 (2013).

[2] S. Goriely *et al.*, Phys. Rev. Lett. **111**, 242502 (2013).

[3] I. V. Panov *et al.*, Nucl. Phys. A **747**, 633 (2005).

[4] M. Eichler *et al.*, The Astrophysical Journal **808**, 30 (2015).

[5] L. Ghys *et al.*, Phys. Rev. C **91**, 044314 (2015).

[6] J. Konki *et al.*, Phys. Lett. B **764**, 265 (2017).

[7] A. N. Andreyev, K. Nishio, and K.-H. Schmidt, Rep. Prog. Phys. **81**, 016301 (2018).

[8] B. Andel *et al.*, β-delayed fission of isomers in ^{188}Bi. Accepted to Phys. Rev. C (2020).

[9] A. N. Andreyev *et al.*, Phys. Rev. Lett. **105**, 252502 (2010).

[10] J. Elseviers *et al.*, Phys. Rev. C **88**, 044321 (2013).

[11] V. Liberati *et al.*, Phys. Rev. C **88**, 044322 (2013).

[12] P. Möller and J. Randrup, Phys. Rev. C **91**, 044316 (2015).

[13] R. Tripathi *et al.*, Phys. Rev. C **92**, 024610 (2015).

[14] I. Tsekhanovich *et al.*, Phys. Lett. B **790**, 583 (2019).

[15] J. G. Cubiss *et al.*, Laser-assisted studies of ^{178}Au. In preparation.

[16] R. D. Harding *et al.*, Laser-assisted decay spectroscopy of ^{176,177,179}Au. In preparation.

[17] M. Veselský *et al.*, Phys. Rev. C **86**, 024308 (2012).

[18] W. D. Myers and W. J. Światecki *et al.*, Phys. Rev. C **60**, 014606 (1999).

[19] P. Möller *et al.*, Phys. Rev. C **79**, 064304 (2009).

[20] M. Wang *et al.*, Chin. Phys. C **41**, 030003 (2017).

[21] A. N. Andreyev *et al.*, IS534 experiment, ISOLDE (2015).

[22] J. G. Cubiss *et al.*, Phys. Lett. B **786**, 355 (2018).

[23] A. E. Barzakh *et al.*, Phys. Rev. C **101**, 034308 (2020).

[24] A. E. Barzakh *et al.*, Shape coexistence in ^{187}Au studied by laser spectroscopy. Submitted to Phys. Rev. C (2020).

[25] A. N. Andreyev *et al.*, Phys. Rev. C **87**, 054311 (2013).

[26] S. Sels *et al.*, Phys. Rev. C **99**, 044306 (2019).

[27] R. D. Harding *et al.*, Mean-square charge radii of gold isotopes. In preparation.

Appendix

DESCRIPTION OF THE PROPOSED EXPERIMENT

The experimental setup comprises: (*name the fixed-ISOLDE installations, as well as flexible elements of the experiment*)

Part of the	Availability	Design and manufacturing
IDS	☒ Existing	☒ To be modified: Addition of annular Si detector for α and fission fragment detection, and $LaBr_3$ detectors for fast-timing measurement
α-decay setup	☒ Existing	☒ To be used without any modification (as designed for IS637)

HAZARDS GENERATED BY THE EXPERIMENT (if using fixed installation:) Hazards named in the document relevant for the fixed IDS installation.

Additional hazards:

Hazards	α-decay setup	[Part 2 of experiment/ equipment]	[Part 3 of experiment/ equipment]
Thermodynamic and fluidic			
Pressure	[pressure][Bar], [volume][l]		
Vacuum	Standard ISOLDE vacuum		
Temperature	[temperature] [K]		
Heat transfer			
Thermal properties of materials			
Cryogenic fluid	[fluid], [pressure][Bar], [volume][l]		
Electrical and electromagnetic			
Electricity	[voltage] [V], [current][A]		
Static electricity			
Magnetic field	[magnetic field] [T]		
Batteries	☐		
Capacitors	☐		
Ionizing radiation			

Target material [C foils]	The C foils where the radioactive samples are implanted are very fragile. Should they break upon opening the α-decay setup, the pieces are so light that they would become airborne. Great care must be taken when opening the system and removing them (slow pumping/venting protective equipment: facial mask).		
Beam particle type (e, p, ions, etc)			
Beam intensity			
Beam energy			
Cooling liquids	[liquid]		
Gases	[gas]		
Calibration sources:	☒		
• Open source	☒		
• Sealed source	☐ [ISO standard]		
• Isotope	^{241}Am		
• Activity	50 Bq		
Use of activated material:			
• Description	☐		
• Dose rate on contact and in 10 cm distance	[dose][mSV]		
• Isotope			
• Activity			
Non-ionizing radiation			
Laser			
UV light			
Microwaves (300MHz-30 GHz)			
Radiofrequency (1-300 MHz)			
Chemical			
Toxic	[chemical agent], [quantity]		
Harmful	[chem. agent], [quant.]		

CMR (carcinogens, mutagens and substances toxic to reproduction)	[chem. agent], [quant.]		
Corrosive	[chem. agent], [quant.]		
Irritant	[chem. agent], [quant.]		
Flammable	[chem. agent], [quant.]		
Oxidizing	[chem. agent], [quant.]		
Explosiveness	[chem. agent], [quant.]		
Asphyxiant	[chem. agent], [quant.]		
Dangerous for the environment	[chem. agent], [quant.]		
Mechanical			
Physical impact or mechanical energy (moving parts)	The chamber of α-decay setup is heavy and needs to be handled with care during installation/removing		
Mechanical properties (Sharp, rough, slippery)	[location]		
Vibration	[location]		
Vehicles and Means of Transport	[location]		
Noise			
Frequency	[frequency],[Hz]		
Intensity			
Physical			
Confined spaces	[location]		
High workplaces	[location]		
Access to high workplaces	[location]		
Obstructions in passageways	[location]		
Manual handling	[location]		
Poor ergonomics	[location]		

Hazard identification:

Average electrical power requirements (excluding fixed ISOLDE-installation mentioned above): negligible